and Korea Science and Engineering Foundation.

References

(1) A. Rossi and C. W. David and R. Schor, *Theoret. Chim. Acta.*, **14**, 429 (1969).

(2) E. Wiberg and R. Bauer, *Z. Naturforsch.*, **6b**, 171 (1951).

(3) R. Ahlrichs and W. Kutzelnigg, *Theoret. Chim. Acta. (Berl)*, **10**, 377 (1968).

(4) P. H. Geil, "Polymer Single Crystals," Interscience, New York, 1963.

(5) H. D. Keith, "Physics and Chemistry of the Organic Solid State," Vol. I, Interscience, New York, 1963.

(6) J. M. Andre and G. Leroy, *Chem. Phys. Lett.*, **5,** 71 (1970).

(7) J. M. Andre, G. S. Kapsomenos and G. Leroy, *Chem. Phys. Lett.*, **8**, 195 (1971).

(8) J. M. Andre and J. Delhalle, *Chem. Phys. Lett.*, **17**, 145 (1972).

(9) K. Morokuma, *Chem. Phys. Lett.*, **6**, 186 (1970).

(10) H. Fujita and A. Imamura, *J. Chem. Phys.*, **53**, 4555 (1970).

(11) G. Morosi and M. Simonetta, *Chem. Phys. Lett.*, **8**, 358 (1971).

(12) K. Morokuma, *J. Chem. Phys.*, **54**, 1962 (1971).

(13) J. M. Andre, J. Delhale, G. S. Kapsomenos and G. Leroy, *Chem. Phys. Lett.*, **14**, 485 (1972).

(14) B. J. McAloon and P. G. Perkins, *Faraday Discuss.*, **II,** 1121 (1971).

(15) J. A. Pople, D. P. Santry and G. A. Segal, *J. Chem. Phys.*, **43**, S129, S136 (1965).

(16) J. A. Pople and G.A. Segal, *J. Chem. Phys.*, **44**, 3289 (1966)

(17) J. A. Pople and D. L. Boveridge, "Approximate Molecular Orbital Theory," McGraw–Hill, New York (1970).

(18) K. T. No. and M. S. Jhon, *J. Phys. Chem.*, **87**, 226 (1983).

(19) J. S. Kim, K. J. No and M. S. Jhon, Sumitted to J. Phys. Chem.

(20) J. Bacon and D. P. Santry, J. Chem. Phys., **56**, 2011 (1972).

(21) R. David and G. Perkins, *Theoret. Chim. Acta.* (Berl), **51,** 163(1979).

(22) S. Kavesh and J. M. Schultz, *J. Polym. Sci., Part A-2,* **8**, 243(1970).

(23) T. Yemni and R. L. McCullough, *J. Polym. Sci., Part A-2,* **11**, 1385 (1973).

Kinetics and Mechanisms of the Oxidation of Carbon Monoxide on Ni–Doped α–Fe$_2$O$_3$

Keu Hong Kim, Jong Ho Jun and Jae Shi Choi

Department of Chemistry, Yonsei University, Seoul 120, Korea (Received September 15, 1983)

The oxidation of carbon monoxide has been investigated on Ni–doped α–Fe$_2$O$_3$ catalyst at 300 to 450 °C. The oxidation rates have been correlated with 1.5–order kinetics; first with respect to CO and 1/2 with respect to O$_2$. Carbon monoxide is adsorbed on lattice oxygen of Ni–doped α–Fe$_2$O$_3$, while oxygen appears to be adsorbed on oxygen vacancy formed by Ni–doping. The conductivities show that adsorption of CO on O–lattice produces conduction electron and adsorption of O$_2$ on O–vacancy withdraws the conduction electron from vacancy. The adsorption process of CO on O–lattice is rate–determining step and dominant defect of Ni–doped α–Fe$_2$O$_3$ is suggested from the agreement between kinetic and conductivity data.

Introduction

A classification of solid catalysts based on electronic properties was formally announced by Dowden.[1] This classification sorted out catalysts into three distinct groups: (a) Conductors (metals), (b) Semiconductors (metal oxides and sulphides) and (c) Insulators (refractory oxides). From the standpoint of widespread application as catalysts, extrinsic semiconductors, which owe their electrical conductance to defect lattice structure of nonstoichiometry or both, are of absorbing interest. Nonstoichiometry may arise out of the incorporation of extra atoms into the crystal at interstitial sites or due to the vacancies caused by the absence of atoms from normal sites. Oxygen vacancies in ZnO are due to excess Zn dissolved in the interstitial sites of ZnO.[2] On the other hand, oxygen

deficiency in ZnO is due to excess Zn which can be dissolved in the interstitial sites of ZnO.[3-7]
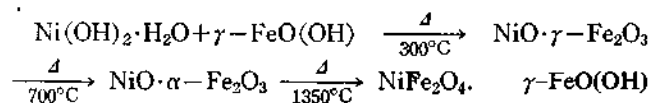
The catalytic properties of a semiconductor, such as its specificity and activity for a particular reaction, are strongly dependent upon its electronic properties. This is strikingly demonstrated by the effect of doping on the electrical and catalytic properties of the semiconductor. The systematic studies of Schwab and Block[8] on the oxidation of CO on Li– and Cr–doped NiO and on Li– and Ga–doped ZnO provide suitable examples to illustrate this correlation.

On a α–Fe$_2$O$_3$ catalyst, it was reported that an Fe$_i^{2+}$ interstitial and an oxygen vacancy might be required to adsorb CO and O$_2$[9]. Ni–doped α–Fe$_2$O$_3$, however, the catalyst used in this work shows that CO is adsorbed on lattice oxygen of Ni–doped α–Fe$_2$O$_3$, while O$_2$ appears to be adsorbed on

oxygen vacancy formed by Ni–doping.

Experimental Section

Material Preparation. 8 mol % Ni-doped α-Fe$_2$O$_3$ powder and pellet. The catalyst was prepared by the following chemical reaction:

$$Ni(OH)_2 \cdot H_2O + \gamma - FeO(OH) \xrightarrow[300°C]{\Delta} NiO \cdot \gamma - Fe_2O_3$$

$$\xrightarrow[700°C]{\Delta} NiO \cdot \alpha - Fe_2O_3 \xrightarrow[1350°C]{\Delta} NiFe_2O_4. \qquad \gamma - FeO(OH)$$

was prepared from NaNO$_2$ and Fe(OH)$_2$ which was precipitated from chemically extra pure FeCl$_2$·4H$_2$O and (CH$_2$)$_6$N$_4$. X-ray diffraction patterns showed that Fe$_2$O$_3$ prepared by the above procedure is α-Fe$_2$O$_3$.

In order to measure the conductivity, Ni-doped α-Fe$_2$O$_3$ powder was made into a pellet under a pressure of 2 tons/cm^2 and sintered at 400°C for 2 hours and then cooled rapidly to room temperature. The pellets were given a light abrasive polish on both faces until voids of the interface region were fully eliminated. The specimens were cut into a cube 0.5×0.7 ×0.18 cm^3. Before the sample was inserted into the sample container, it was etched in (NH$_4$)$_2$S$_2$O$_8$ and dilute HNO$_3$, and washed with distilled water, and then dried.

CO: Carbon monoxide was prepared by the reaction of CaCO$_3$ and Zn powder.[10] The reaction was carried out by heating to 800°C. CO was purified with glass wool, KOH, CaCl$_2$, and P$_2$O$_5$, and stored in a container which had been evacuated to 1×10^{-5} torr.

O$_2$: Oxygen obtained by heating potassium chlorate at about 600°C was purified by passing it over glass wool, P$_2$O$_5$, and CaCl$_2$.

The analyses of the reactant gases CO and O$_2$ were carried out by methods described elsewhere.[9]

Apparatus and Procedure. Details of the experimental apparatus and procedure have been given in previous studies.[2,9,11] In this work 200 ml was total volume of the reaction and the fixed amount of catalyst (100-160 mesh) was 0.5 g. The catalyst was etched in d-HNO$_3$ solution, washed with distilled water, dried in an oven, and sintered at 400°C under 1×10^{-5} torr. The total initial pressure of the stoichiometric reactant mixture (CO+1/2 O$_2$) was 225 torr.

Results

The kinetic data for CO oxidation on Ni-doped α-Fe$_2$O$_3$ were found to obey closely the expression $-dp/dt = kP^{1.5}$ with respect to the total pressure $(P = P_{CO} + P_{O_2} = 225$ torr) in the reaction temperature range of 300 to 450°C; 1.5 order was confirmed by a graphical method leading to a linear plot.

Figure 1 shows $10^3/2(P^{-0.5} - P_0^{-0.5})$ plotted against time at reaction temperatures of 300 to 450°C, the linearity confirming 1.5-order kinetics. The rate constants are listed in Table 1 and found to be compatible with the Arrhenius equation.

Figure 2 shows the logarithm of the rate constant plotted against the reciprocal of the absolute temperature. The slope of the line was calculated from the plot, and the activation energy was found to be 11.5 kcal/mole for Ni-doped α-Fe$_2$O$_3$ catalyst.
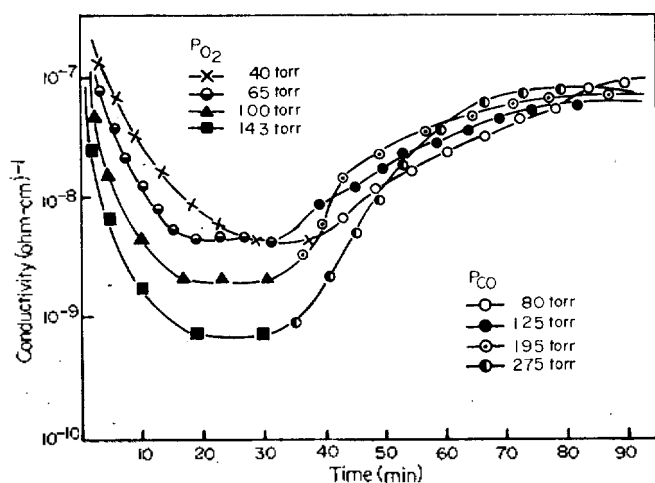
In order to check the influence of partial pressures of CO
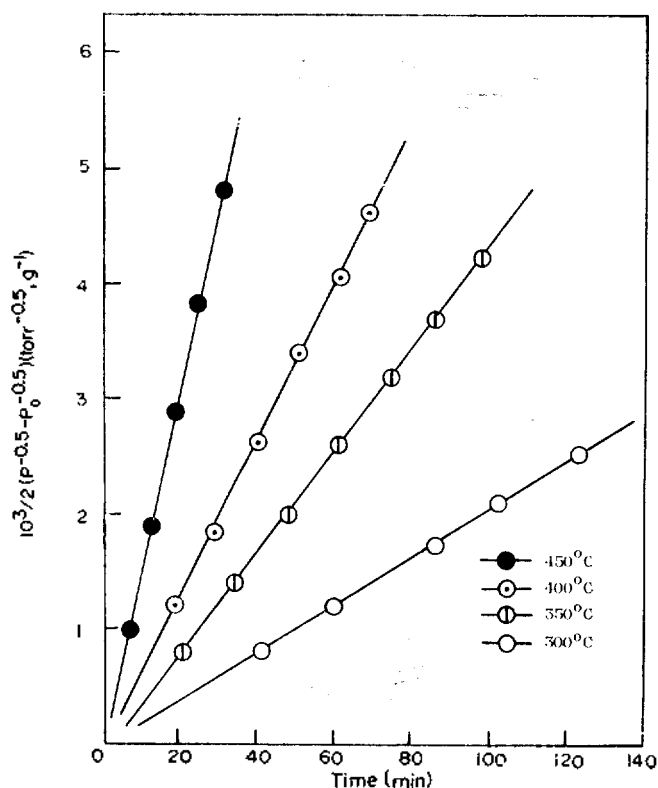
Figure 1. Oxidation rates of CO on Ni-doped α-Fe$_2$O$_3$ at temperatures from 300 to 450 °C. $P_{CO} = 150$torr; $P_{O_2} = 75$torr; Catalyst=0.5g; P=total pressure; P_0=total initial pressure.
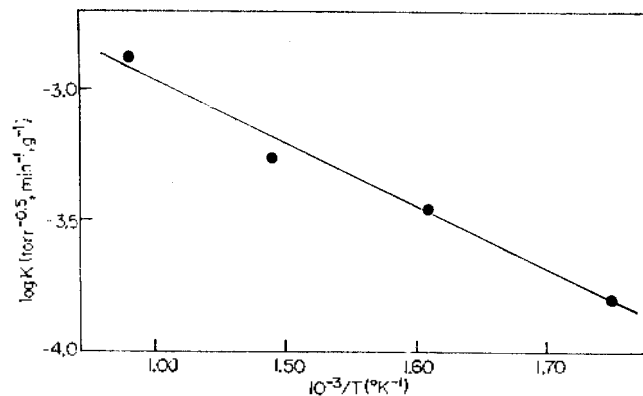
Figure 2. Arrhenius plot for the oxidation of CO on Ni–doped α-Fe$_2$O$_3$.

Figure 3. Conductivity changes of Ni-doped α-Fe$_2$O$_3$ under O$_2$ and after introduction of CO as a function of time at 450 °C.
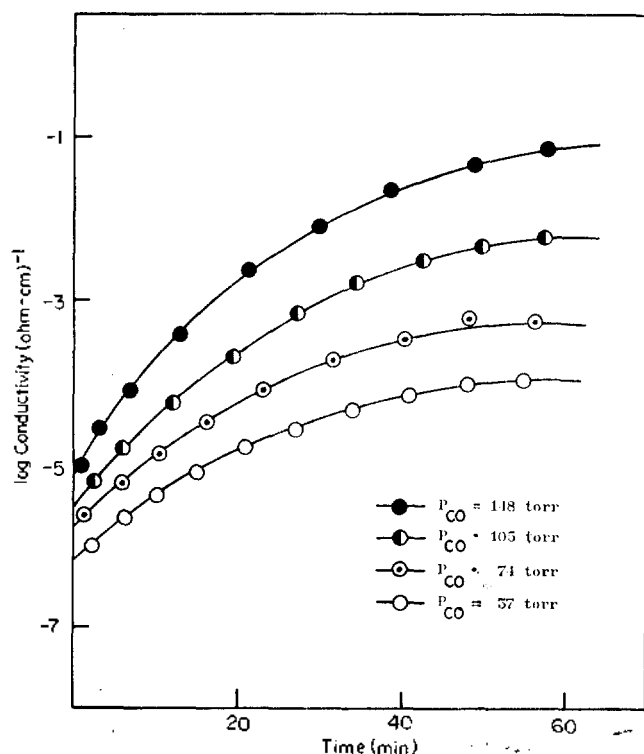
Figure 4. Electrical conductivities of Ni–doped α-Fe$_2$O$_3$ under various partial pressures of CO as a function of time at 400 °C.

TABLE 1: Rate Constants of CO Oxidation on Ni-Doped α-Fe$_2$O$_3$

$T(^\circ C)$	$1/T \times 10^3$	$2\,k(\text{torr}^{-0.5}, \text{g}^{-1}, \text{min}^{-1})$
300	1.75	1.60×10^{-4}
350	1.61	3.57×10^{-4}
400	1.49	5.33×10^{-4}
450	1.38	1.33×10^{-3}

TABLE 2: Reaction Rate Effect of P_{CO} and P_{O_2} for the CO Oxidation on Ni-Doped α-Fe$_2$O$_3$

$T(^\circ C)$	P_{O_2}	P_{CO}	$2V$ (torr, g^{-1}, min^{-1})
300	74	148	0.57
300	38	75	0.19
300	38	150	0.40
450	75	149	3.69
450	37	74	1.36
450	37	150	2.58

and O_2 on the oxidation rates of CO, the ratio of P_{CO} and P_{O_2} was varied. Table 2 shows the exponents of the dependence on P_{CO} and P_{O_2}. The evaluated partial orders were found to be 1 for CO and 0.5 for O_2 on Ni-doped α-Fe$_2$O$_3$.

The electrical conductivity data for Ni–doped α-Fe$_2$O$_3$ in the presences of O_2 and CO are shown in Figures 3 and 4. Figure 3 shows that the conductivity changes with variations of P_{O_2} and P_{CO} as a function of time. The conductivities decrease with O_2, and after increase with CO. Figure 4 shows that the conductivities increase with increasing partial pressures of CO.

Discussion

Figure 1 indicates that the Ni–doped α-Fe$_2$O$_3$ has a cataly-

tic activity above 300°C in the oxidation of CO. The activation energy of 11.5 kcal/mol means that the adsorption of reactants on a Ni–doped α-Fe$_2$O$_3$ catalyst appears to include chemisorption. The 0.5 order with respect to O_2 suggests that O_2 adsorbs into two species, ie., ionic oxygen atoms.

On the other hand, the conductivity data shown in Figure 3 show that CO does not adsorb on an oxygen vacancy; the increased conductivities with increasing partial pressures of CO indicate that the chemisorption of CO produces conduction electrons. If CO is adsorbed on an oxygen vacancy, the electrical conductivity should decrease with increasing CO partial pressures. This means that the adsorption of CO on oxygen vacancies reduces the concentration of conduction electrons trapped at oxygen vacancies formed by Ni-doping. Therefore, one can see that the oxygen vacancy is not the site involved in the adsorption of CO and must consider another site.

If the lattice oxygen is a possible site for adsorption of CO, the electrical conductivity should increase according to the following equilibrium,

$$CO + O^{2-}_{(latt)} \overset{K_1}{\rightleftharpoons} CO^-_{2(ads)} + e^- \qquad (1)$$
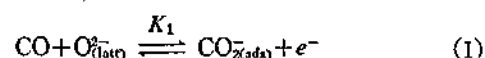
where $O^{2-}_{(latt)}$ is a lattice oxygen in Ni–doped α-Fe$_2$O$_3$ and $CO^-_{2(ads)}$ is a carbon monoxide which is adsorbed on a lattice oxygen. Equilibrium (1) is consistent with the experimental result shown in Figure 4, and therefore the lattice oxygen is a adsorption site of CO.

If O_2 adsorbs on an oxygen vacancy, the electrical conductivity should decrease according to the following equilibrium

$$2e^- + O_2 \overset{K_2}{\rightleftharpoons} 2O^-_{(ads)} \qquad (2)$$
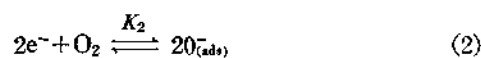
where e^- is considered as a conduction electron trapped at an oxygen vacancy formed by Ni-doping. This suggested equilibrium is consistent with the experimental result in Figure 3.

The kinetic data shown in Table 2 show that the reaction rates increase with increasing P_{CO} and P_{O_2}. This result indicates that the equilibria (1) and (2) proceed to the right and the elementary reaction (3) may be involved in the oxidation of CO.

$$CO^-_{2(ads)} + O^-_{(ads)} \overset{k}{\longrightarrow} CO_2 + O^{2-}_{(latt)} \qquad (3)$$
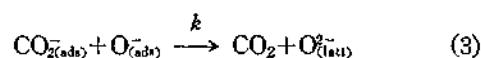
The conductivity data in Figure 3 is consistent with the kinetic data in Table 2, if the formations of $CO^-_{2(ads)}$ and $O^-_{(ads)}$ contribute to the oxidation of CO.

With above informations, one can show that the suggested mechanism leads to the observed rate law. Experimental rate law is $-dp/dt = kP_{O_2}^{1/2}\,P_{CO}$; first with respect to CO and 1/2 with respect to O_2.

From equation 2, $(O^-_{(ads)}) = (K_2)^{1/2}\,(e^-)\,(O_2)^{1/2}$, and from equation 1, $(CO^-_{2(ads)}) = K_1 \dfrac{(CO)(O^{2-}_{(latt)})}{(e^-)}$. From equation 3, the rate of production of CO_2 can be represented as followings:
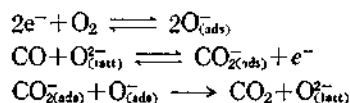
$$\frac{d(CO_2)}{dt} = k\,(CO^-_{2(ads)})\,(O^-_{(ads)}) \qquad (4)$$

Substituting $(CO^-_{2(ads)}) = K_1\,(CO)\,(O^{2-}_{(latt)})/(e^-)$ and $(O^-_{(ads)}) =

$(K_2)^{1/2}(e^-)\ (O_2)^{1/2}$ into equation (4), the rate equation can be rewritten as follows:

$$\frac{d(CO_2)}{dt} = k\,K_1\frac{(CO)\,(O^{2-}_{(latt)})}{(e^-)}K_2^{1/2}(e^-)\,(O_2)^{1/2}$$
$$= k\,K_2^{1/2}\,K_1(CO)\,(O_2)^{1/2}(O^{2-}_{(latt)})$$
$$= k'\,(CO)\,(O_2)^{1/2}$$

Thus, the suggested mechanism leads to the observed rate law, first order with respect to CO and 0.5 with respect to O_2. Therefore, the oxidation mechanism of CO on Ni-doped α-Fe_2O_3 can be suggested as follows:

$$2e^- + O_2 \rightleftharpoons 2O^-_{(ads)}$$
$$CO + O^{2-}_{(latt)} \rightleftharpoons CO^-_{2(ads)} + e^-$$
$$CO^-_{2(ads)} + O^-_{(ads)} \longrightarrow CO_2 + O^{2-}_{(latt)}$$

With the conductivity data shown in Figures 3 and 4, we can find that the rate determining step is the chemisorption of CO on a lattice oxygen.

Acknowledgement. The authors are grateful to the Korean Trader's Scholarship Foundation for financial support.

References

(1) D. A. Dowden, *J. Chem. Soc.* **242** (1950).

(2) J. S. Choi, K. H. Kim and S. R. Choi, *Inter. J. Chem. Kinetics* **9,** 489 (1977).

(3) J. H. Boer, "Reactivity of Solids," Elsevier, Amsterdam, 381, 1961.

(4) F. A. Kröger, "Chemistry of Imperfect Crystals," North Holland Publishing Co., Amsterdam, 692, 1970.

(5) B. M. Arghiropoulos and S. J. Teichner, *J. Catal.* **3,** 477 (1964).

(6) H. Z. Chon and C. D. Prater, *Discuss Faraday Soc.,* **41,** 380 (1966).

(7) H. Krebs, "Fundamentals of Inorganic Crystal Chemistry," McGraw-Hill, London, 162, 1968.

(8) G. M. Schwab and J. Block, *Z. Physik. Chem. N.F.,* **1,** 42 (1954); *Z. Electrochem,* **58,** 756 (1954).

(9) K. H. Kim, H. S. Han and J. S. Choi, *J. Phys. Chem,* **83,** 1286 (1979).

(10) S. Weinhouse, *J. Amer. Chem. Soc. Commun. Edu.,* **70,** 442 (1948).

(11) J. S. Choi, Y. H. Kang and K. H. Kim, *J. Phys. Chem.,* **81,** 2208 (1977).

A Study of the Ionic Association of the Substituted N-Methyl Pyridinium Iodides (I). N-Methyl Pyridinium Iodide in Ethanol-Water Mixture

Jong Gi Jee and Oh Cheun Kwun[†]

Department of Chemistry, Hanyang University, Seoul 133, korea (Received August 18, 1983)

The ionic association constant (K) of N-methyl pyridinium iodide (NMPI) ion in several ethanol-water mixtures were determined by the combination of UV spectroscopy and conductance measurements using the Shedlovsky function as a correction factor. The measurement of electrical conductance and UV absorption were performed in 95, 90, 80 and 60 volume percentages of ethanol in the solvent mixture at 15, 25, 35 and 45 (± 0.1) °C. The ion size parameter ($r_{A^+D^-}$) and the dipole moment ($\mu_{A^+D^-}$) of NMPI ion were obtained from the linear plots of ln K vs. $(1/D)$ and $(D-1)/(2D+1)$, respectively. These $\mu_{A^+D^-}$ values were in good agreement with the values of transition moment calculated from the equation, $\mu_{nm} = 6.5168 \times 10^{-2} \times \left(\epsilon_{max}\frac{\bar{\nu}_{\frac{1}{2}}}{\bar{\nu}_{max}}\right)^{\frac{1}{2}}$ (Debye) which we have derived. The thermodynamic parameters indicate (1) that the water dipoles have an ordered rearrangement around the dipolar NMPI ions rather than the configuration existing in bulk free waters; and (2) that the equilibrium state between NMPI ion and its component ions are controlled by entropy.

Introduction

It has been observed by Kosower[1,2] that N-methyl pyridinium iodide(NMPI) gives rise to an ultraviolet charge transfer band in aqueous solution. This band arises due to a transfer of electron density from an occupied orbital of iodide into the lowest unoccupied orbital of the pyridinium ion.[3-5] Subsequently, it was shown that the concentration dependence of the charge transfer band could be employed to calculate the association constants (K) for the equilibrium state in which N-methyl pyridinium cation and iodide anion associated to form the N-methyl pyridinium iodide dipolar ion complex.

Paul Hemmes *et al.* have investigated the equilibrium and kinetics for the association of NMPI in water-alcohol mixtures by the combination of UV spectroscopy and conductance measurements using the Fuoss function as a correction factor.[6] These authors have not studied the thermodynamic variables, dipole moment and radius of the dipolar NMPI ion.

Therfore, we studied the ionic association of NMPI in ethanol-water mixture by a combination of UV spectroscopy and conductance measurements using the Shedlovsky func-